PHYSICAL REVIEW D **83,** 075016 (2011)

Triviality and vacuum stability bounds in the three-loop neutrino mass model

Mayumi Aoki,[1,*] Shinya Kanemura,[2,†] and Kei Yagyu[2,‡]

[1]*Institute for Theoretical Physics, Kanazawa University, Kanazawa 920-1192, Japan*
[2]*Department of Physics, University of Toyama, 3190 Gofuku, Toyama 930-8555, Japan*

(Received 16 February 2011; published 25 April 2011)

We study theoretical constraints on the parameter space under the conditions from vacuum stability and triviality in the three-loop radiative seesaw model with TeV-scale right-handed neutrinos which are odd under the Z_2 parity. In this model, some of the neutrino Yukawa coupling constants can be of the order of 1. The requirement of a strongly first order phase transition for successful electroweak baryogenesis also prefers order-one coupling constants in the scalar sector. Hence, it is important to clarify whether this model satisfies those theoretical conditions up to a given cutoff scale. It is found that the model can be consistent up to the scale above 10 TeV in the parameter region where the neutrino data, the lepton-flavor violation data, the thermal relic abundance of dark matter as well as the requirement from the strongly first order phase transition are satisfied.

DOI: 10.1103/PhysRevD.83.075016 PACS numbers: 12.60.Fr, 14.60.St

I. INTRODUCTION

The Higgs sector is the last unknown part in the standard model (SM). There is no compelling reason that it takes its minimal form. Instead, there can be various possibilities for nonminimal Higgs sectors. Currently, searches for the Higgs boson are under way at the Tevatron and the Large Hadron Collider (LHC). It is expected that crucial information for the Higgs sector will be obtained in the near future. On the other hand, there are phenomena which cannot be explained within the SM such as neutrino oscillation, existence of dark matter, and baryon asymmetry of the Universe. They provide us strong motivations to consider physics beyond the SM.

The Higgs sector may be related to the physics to cause these phenomena. First of all, based on the weakly interacting massive particle (WIMP) hypothesis, the observed value of the relic abundance requires the mass of the dark matter to be around the electroweak scale. Why is the mass of the WIMP dark matter at the electroweak scale? This would strongly indicate a direct connection between the WIMP dark matter and the Higgs sector [1,2]. Second, the origin of neutrino masses may also be the TeV scale: i.e., the origin of the lepton number violation would be the existence of TeV-scale right-handed neutrinos or that of lepton number violating scalar interactions in the extended Higgs sector. As a natural scenario for generating tiny neutrino masses, such lepton number violation at the TeV scale would be transmitted to the left-handed neutrino sector via loop effects of the Higgs sectors. This is the so-called the radiative seesaw scenario [3–7]. Finally, a simple description of baryon asymmetry of the Universe may be the scenario in which electroweak phase transition is of strong first order in order to satisfy the Sakharov's condition of departure from thermal equilibrium [8]. This is the scenario of electroweak baryogenesis [9].

An attractive point for these scenarios would be that they can give definite predictions to TeV-scale phenomenology, so that we can directly test them by experiments, in principle. Various scenarios for the WIMP dark matter can be tested by direct and indirect searches as well as collider experiments [1,2,10]. Each radiative seesaw model predicts a characteristic extended Higgs sector with lepton number violating interactions [3,4,11–13] or right-handed neutrinos [5,6,14–16]. It is known that the dynamics for the electroweak baryogenesis is strongly related to the Higgs boson phenomenology at colliders [17].

Therefore, an interesting question is whether or not we can construct a *successful* TeV-scale phenomenological model where these three phenomena would be explained simultaneously. Recently, a TeV-scale model has been proposed for such a purpose [7], in which (1) tiny neutrino masses are generated without excessive fine-tuning at the three-loop level by the dynamics of an extended Higgs sector and right-handed neutrinos under an unbroken Z_2 parity, (2) the Z_2 parity also guarantees the stability of a dark matter candidate which is a Z_2 odd scalar boson, and (3) the strongly first order phase transition for successful electroweak baryogenesis can be realized by the nondecoupling effect in the Higgs sector. Phenomenology of this model has been discussed in Ref. [18], and the related collider physics [19–21] and dark matter properties [22] have also been studied. In these papers, phenomenologically allowed parameter regions have been mainly discussed.

In this paper, we investigate the theoretical constraint on the parameter regions in this model [7] from the requirement of vacuum stability and perturbativity up to a given cutoff scale Λ of the model [23]. In the present model, there is no mechanism for cancellation of the quadratic

*mayumi@hep.s.kanazawa-u.ac.jp
†kanemu@sci.u-toyama.ac.jp
‡keiyagyu@jodo.sci.u-toyama.ac.jp

divergences which appear in the renormalization calculation for the Higgs boson mass, so that a huge fine-tuning is required if Λ is much higher than the electroweak scale. To avoid such an unnatural situation, we need to consider Λ to be at most $\mathcal{O}(10)$TeV, above which the model would be replaced by a more fundamental theory [24]. Hence, we have to study the theoretical consistency of the model up to such values for Λ. In particular, some of the neutrino Yukawa coupling constants are of order one in magnitude, as the scale of tiny neutrino masses is generated by loop dynamics so that we do not need fine-tuning for the size of the coupling constants. In addition, some of the coupling constants in the Higgs potential are of order one to realize the nondecoupling one-loop effect for strongly first order phase transition. Although the parameters discussed in the previous works satisfy the bound from tree-level unitarity [25], it is nontrivial that the model can be consistent at the quantum level with the theoretical requirements up to $\Lambda \sim 10$ TeV. Theoretical bounds from vacuum stability and perturbativity have been used to constrain parameters in extended Higgs sectors such as the two Higgs doublet model [26] and the Zee model [11]. Here we apply the similar analysis to the model. We prepare a full set of the renormalization group equations (RGEs) for dimensionless coupling constants in the model at the one-loop level, and analyze the behavior of running coupling constants.

We also revise the phenomenological constraint from lepton-flavor violation (LFV) in the model. In the previous analysis [7,18], only the constraint from $\mu \to e\gamma$ data has been taken into account. Here, we also analyze the one-loop induced $\mu \to eee$ process, whose current experimental data [27] turn out to give a stronger bound on the parameter space than those of $\mu \to e\gamma$ [28].

The paper is organized as follows. In Sec. II, we give a brief review of the model. In Sec. III, we introduce the criteria for vacuum stability and triviality, and numerical results of the RGE analysis are presented. In Sec. IV, we give a conclusion.

II. THE THREE-LOOP NEUTRINO MASS MODEL

We give a short review for the three-loop neutrino mass model in Ref. [7] to make the paper self-contained.

A. Model

In this model, two Higgs doublets (Φ_1 and Φ_2) with hypercharge $Y = 1/2$, charged scalar singlets ($S^{\pm}$), a real scalar singlet (η), and right-handed neutrinos (N_R^α with $\alpha = 1, 2$) are introduced. We impose two kinds of discrete symmetries; i.e., Z_2 and $\tilde{Z}_2$ to the model. The former, which is exact, is introduced in order to forbid the tree-level Dirac neutrino mass term and at the same time to guarantee the stability of dark matter. The latter one, which is softly broken, is introduced to avoid the tree-level flavor changing neutral current [29]. Under the $\tilde{Z}_2$ symmetry there are four types of Yukawa interactions [30,31]. In our model [7], the so-called type-X Yukawa interaction [19,32] is favored since the charged Higgs boson from the two doublets can be taken to be as light as around 100 GeV without contradicting the $b \to s\gamma$ data. Such a light charged Higgs boson is important to reproduce the correct magnitude of neutrino masses. The particle properties under the discrete symmetries are shown in Table I, where Q_L^i, u_R^i, d_R^i, L_L^i, and e_R^i are the ith generation of the left-handed quark doublet, the right-handed up-type quark singlet, the left-handed lepton doublet, and the right-handed charged lepton singlet, respectively.

The type-X Yukawa interaction is given by

$$\mathcal{L}_{\text{Yukawa}}^{\text{type-X}} = -\sum_{i,j}[(\bar{Q}_L^i Y_{ij}^d \Phi_2 d_R^j) + (\bar{Q}_L^i Y_{ij}^u \Phi_2^c u_R^j) + (\bar{L}_L^i Y_{ij}^e \Phi_1 e_R^j)] + \text{H.c.}, \tag{1}$$

where Yukawa coupling matrix for leptons is diagonal, $Y_{ij}^e = \text{diag}(y_{e^1}, y_{e^2}, y_{e^3})$. The mass term and the Yukawa interaction for N_R^α are written as

$$\mathcal{L}_{N_R} = \sum_{\alpha=1}^{2} \frac{1}{2} m_{N_R^\alpha} \overline{(N_R^\alpha)^c} N_R^\alpha - \sum_{i=1}^{3}\sum_{\alpha=1}^{2} [h_i^\alpha \overline{(e_R^i)^c} N_R^\alpha S^+ + \text{H.c.}]. \tag{2}$$

The scalar potential is given by

$$\begin{aligned} V = {} & +\mu_1^2|\Phi_1|^2 + \mu_2^2|\Phi_2|^2 - [\mu_3^2 \Phi_1^\dagger \Phi_2 + \text{H.c.}] + \frac{1}{2}\lambda_1|\Phi_1|^4 + \frac{1}{2}\lambda_2|\Phi_2|^4 + \lambda_3|\Phi_1|^2|\Phi_2|^2 + \lambda_4|\Phi_1^\dagger \Phi_2|^2 \\ & + \frac{1}{2}[\lambda_5(\Phi_1^\dagger \Phi_2)^2 + \text{H.c.}] + \mu_S^2|S^-|^2 + \rho_1|S^-|^2|\Phi_1|^2 + \rho_2|S^-|^2|\Phi_2|^2 + \frac{1}{4}\lambda_S|S^-|^4 + \frac{1}{2}\mu_\eta^2\eta^2 + \frac{1}{2}\sigma_1\eta^2|\Phi_1|^2 \\ & + \frac{1}{2}\sigma_2\eta^2|\Phi_2|^2 + \frac{1}{4!}\lambda_\eta\eta^4 + \sum_{a,b=1}^{2}[\kappa\epsilon_{ab}(\Phi_a^c)^\dagger \Phi_b S^- \eta + \text{H.c.}] + \frac{1}{2}\xi|S^-|^2\eta^2, \end{aligned} \tag{3}$$

where ϵ_{ab} are antisymmetric matrices with $\epsilon_{12} = 1$. The parameters μ_3^2, λ_5, and κ are complex numbers. Two of their phases can be absorbed by rephasing the fields, and the rest is a physical one. In this paper, we neglect this CP-violating phase for simplicity. The Higgs doublets are parametrized as

TABLE I. Particle properties under the discrete symmetries.

	$Q_L^i u_R^i d_R^i L_L^i e_R^i$	$\Phi_1\Phi_2$	$S^\pm \eta N_R^\alpha$
Z_2 (exact)	+ + + + +	++	− − −
$\tilde{Z}_2$ (softly broken)	+ − − + +	+−	+ − +

$$\Phi_i = \begin{pmatrix} w_i^+ \\ \frac{1}{\sqrt{2}}(h_i + v_i + iz_i) \end{pmatrix}, \tag{4}$$

where v_i are vacuum expectation values (VEVs) of the Higgs fields, and these are constrained by $v(=\sqrt{v_1^2+v_2^2}) \simeq 246$ GeV. The ratio of the two VEVs is defined by $\tan\beta = v_2/v_1$. The physical scalar states h, H, A, and $H^\pm$ in the Z_2 even sector can be obtained mixing angles α and β,

$$\begin{aligned} \begin{pmatrix} w_1^\pm \\ w_2^\pm \end{pmatrix} &= R(\beta)\begin{pmatrix} w^\pm \\ H^\pm \end{pmatrix}, \\ \begin{pmatrix} z_1 \\ z_2 \end{pmatrix} &= R(\beta)\begin{pmatrix} z \\ A \end{pmatrix}, \\ \begin{pmatrix} h_1 \\ h_2 \end{pmatrix} &= R(\alpha)\begin{pmatrix} H \\ h \end{pmatrix}, \end{aligned} \tag{5}$$

where $w^\pm$ and z are the Nambu-Goldstone bosons absorbed by the longitudinal weak gauge bosons, and the rotation matrix with the angle θ is given by

$$R(\theta) = \begin{pmatrix} \cos\theta & -\sin\theta \\ \sin\theta & \cos\theta \end{pmatrix}. \tag{6}$$

The mass formulas of physical scalar states are given by

$$m_A^2 = M^2 - v^2\lambda_5, \tag{7}$$

$$m_{H^\pm}^2 = M^2 - \frac{v^2}{2}(\lambda_4+\lambda_5), \tag{8}$$

$$\begin{aligned} m_H^2 = {} & \cos^2(\alpha-\beta)M_{11}^2 + 2\sin(\alpha-\beta)\cos(\alpha-\beta)M_{12}^2 \\ & + \sin^2(\alpha-\beta)M_{22}^2, \end{aligned} \tag{9}$$

$$\begin{aligned} m_h^2 = {} & \sin^2(\alpha-\beta)M_{11}^2 - 2\sin(\alpha-\beta)\cos(\alpha-\beta)M_{12}^2 \\ & + \cos^2(\alpha-\beta)M_{22}^2, \end{aligned} \tag{10}$$

$$m_S^2 = \mu_S^2 + \frac{v^2}{2}\rho_1\cos^2\beta + \frac{v^2}{2}\rho_2\sin^2\beta, \tag{11}$$

$$m_\eta^2 = \mu_\eta^2 + \frac{v^2}{2}\sigma_1\cos^2\beta + \frac{v^2}{2}\sigma_2\sin^2\beta, \tag{12}$$

where $M(=\mu_3/\sqrt{\sin\beta\cos\beta})$ is the soft breaking scale for the $\tilde{Z}_2$ symmetry, and

$$M_{11}^2 = v^2(\lambda_1\cos^4\beta + \lambda_2\sin^4\beta) + \frac{v^2}{2}\lambda\sin^2 2\beta, \tag{13}$$

$$M_{22}^2 = M^2 + v^2\sin^2\beta\cos^2\beta(\lambda_1+\lambda_2-2\lambda), \tag{14}$$

$$M_{12}^2 = v^2\sin\beta\cos\beta(-\lambda_1\cos^2\beta + \lambda_2\sin^2\beta + \lambda\cos 2\beta), \tag{15}$$

with $\lambda = \lambda_3+\lambda_4+\lambda_5$. Notice that M, μ_S, and μ_η are free mass parameters irrelevant to the electroweak symmetry breaking.

B. Neutrino mass and mixing

The neutrino mass matrix M_{ij}^ν is generated by the three-loop diagrams in Fig. 1. The absence of lower order loop contributions is guaranteed by the Z_2 symmetry. The resulting mass matrix is calculated as

$$M_{ij}^\nu = \sum_{\alpha=1}^{2} 4\kappa^2\tan^2\beta(y_{\ell_i}^{\rm SM}h_i^\alpha)(y_{\ell_j}^{\rm SM}h_j^\alpha)F(m_{H^\pm}, m_S, m_{N_R^\alpha}, m_\eta), \tag{16}$$

where the loop integral function F is given by

$$\begin{aligned} & F(m_{H^\pm}, m_S, m_N, m_\eta) \\ & = \left(\frac{1}{16\pi^2}\right)^3 \frac{(-m_N)}{m_N^2-m_\eta^2}\frac{v^2}{m_{H^\pm}^4}\int_0^\infty x\,dx\{B_1(-x, m_{H^\pm}, m_S) \\ & \quad - B_1(-x, 0, m_S)\}^2\left(\frac{m_N^2}{x+m_N^2} - \frac{m_\eta^2}{x+m_\eta^2}\right), \end{aligned} \tag{17}$$

with $y_{\ell_i}^{\rm SM} = \sqrt{2}m_{\ell_i}/v$, where ℓ_1, ℓ_2, and ℓ_3 correspond to e, μ, and τ, respectively. The function B_1 is the tensor coefficient in the formalism by Passarino-Veltman for one-loop integrals [33]. In the following discussion, we take $m_{N_R^1} = m_{N_R^2} \equiv m_{N_R}$, for simplicity. Numerically, the magnitude of the function F is of order 10^4 eV in the wide range of parameter regions of our interest. Since $y_{\ell_i}^{\rm SM} < 10^{-2}$, the correct scale of neutrino masses can be naturally obtained from the three-loop diagrams.

The generated mass matrix M_{ij}^ν in Eq. (16) of neutrinos can be related to the neutrino oscillation data by

$$M_{ij}^\nu = U_{is}(M_{\rm diag}^\nu)_{\rm st}(U^T)_{tj}, \tag{18}$$

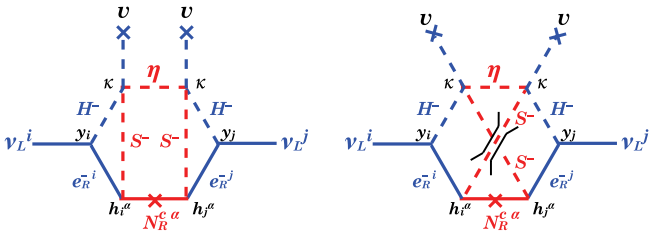

FIG. 1 (color online). The Feynman diagrams for generating tiny neutrino masses.

where $M^{\nu}_{\rm diag} = {\rm diag}(m_1, m_2, m_3)$. For the case of the normal hierarchy we identify the mass eigenvalues as $m_1 = 0$, $m_2 = \sqrt{\Delta m^2_{\rm solar}}$, $m_3 = \sqrt{\Delta m^2_{\rm atm}}$, while for inverted hierarchy $m_1 = \sqrt{\Delta m^2_{\rm atm}}$, $m_2 = \sqrt{\Delta m^2_{\rm atm} + \Delta m^2_{\rm solar}}$, and $m_3 = 0$ are taken. The Maki-Nakagawa-Sakata matrix U_{is} [34] is parametrized as

$$U = \begin{bmatrix} 1 & 0 & 0 \\ 0 & c_{23} & s_{23} \\ 0 & -s_{23} & c_{23} \end{bmatrix} \begin{bmatrix} c_{13} & 0 & s_{13}e^{i\delta} \\ 0 & 1 & 0 \\ -s_{13}e^{-i\delta} & 0 & c_{13} \end{bmatrix} \times \begin{bmatrix} c_{12} & s_{12} & 0 \\ -s_{12} & c_{12} & 0 \\ 0 & 0 & 1 \end{bmatrix} \begin{bmatrix} 1 & 0 & 0 \\ 0 & e^{i\tilde{\alpha}} & 0 \\ 0 & 0 & e^{i\tilde{\beta}} \end{bmatrix}, \tag{19}$$

where s_{ij} and c_{ij} represent $\sin\theta_{ij}$ and $\cos\theta_{ij}$, respectively, with θ_{ij} to be the neutrino mixing angle between the ith and jth generations, and δ is the Dirac phase while $\tilde{\alpha}$ and $\tilde{\beta}$ are Majorana phases. For simplicity, we neglect the effects of these CP violating phases in the following analysis. Current neutrino oscillation data give the following values [35]:

$$\Delta m^2_{\rm solar} \simeq 7.59 \times 10^{-5}\ {\rm eV}^2, \qquad |\Delta m^2_{\rm atm}| \simeq 2.43 \times 10^{-3}\ {\rm eV}^2, \tag{20}$$

$$\sin^2\theta_{12} \simeq 0.32, \qquad \sin^2\theta_{23} \simeq 0.5, \qquad \sin^2\theta_{13} < 0.04. \tag{21}$$

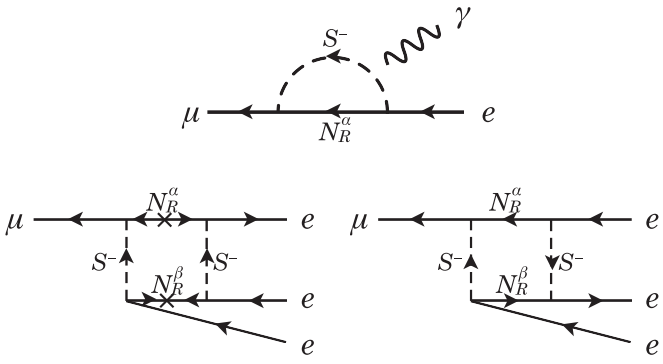

FIG. 2. The LFV processes.

In the next subsection, we discuss parameter regions in which both neutrino data and the LFV data are satisfied.

C. Lepton-flavor violation

The model receives the severe constraints from the lepton-flavor violating processes of $\mu \to e\gamma$ and $\mu \to eee$: see Fig. 2. These processes are induced through one-loop diagrams by N_R^α and $S^\pm$ with the Yukawa couplings h_i^α ($i = e$ and μ). The branching ratio of $\mu \to e\gamma$ is given by[1]

$$B(\mu \to e\gamma) \simeq \frac{3\alpha_{\rm em}v^4}{32\pi m_S^4} \left| \sum_{\alpha=1}^{2} h_e^{\alpha *} h_\mu^\alpha F_2\left(\frac{m^2_{N_R^\alpha}}{m_S^2}\right) \right|^2, \tag{22}$$

where $F_2(x) \equiv (1 - 6x + 3x^2 + 2x^3 - 6x^2\ln x)/6(1-x)^4$. For $\mu \to eee$, the branching ratio is calculated by

$$\begin{aligned} B(\mu \to eee) = {} & \frac{1}{64G_F^2}\left(\frac{1}{16\pi^2}\right)^2 \left| \sum_{\alpha,\beta=1}^{2} \left(\frac{1}{m^2_{N_R^\alpha} - m_S^2}\right)\left(\frac{1}{m^2_{N_R^\beta} - m_S^2}\right) \right. \\ & \times \left[h_\mu^{\alpha *} h_e^\alpha h_e^{\beta *} h_e^\beta \left(\frac{m^2_{N_R^\alpha} m^2_{N_R^\beta}}{m^2_{N_R^\alpha} - m^2_{N_R^\beta}} \log\frac{m^2_{N_R^\alpha}}{m^2_{N_R^\beta}} - \frac{m^2_{N_R^\alpha} m_S^2}{m^2_{N_R^\alpha} - m_S^2} \log\frac{m^2_{N_R^\alpha}}{m_S^2} - \frac{m^2_{N_R^\beta} m_S^2}{m^2_{N_R^\beta} - m_S^2} \log\frac{m^2_{N_R^\beta}}{m_S^2} + m_S^2 \right) \right. \\ & \left. \left. + h_\mu^{\alpha *} h_e^{\alpha *} h_e^\beta h_e^\beta m_{N_R^\alpha} m_{N_R^\beta} \left(-\frac{m^2_{N_R^\alpha} + m^2_{N_R^\beta}}{m^2_{N_R^\alpha} - m^2_{N_R^\beta}} \log\frac{m^2_{N_R^\alpha}}{m^2_{N_R^\beta}} + \frac{m^2_{N_R^\alpha} + m_S^2}{m^2_{N_R^\alpha} - m_S^2} \log\frac{m^2_{N_R^\alpha}}{m_S^2} + \frac{m^2_{N_R^\beta} + m_S^2}{m^2_{N_R^\beta} - m_S^2} \log\frac{m^2_{N_R^\beta}}{m_S^2} - 2 \right) \right] \right|^2. \end{aligned} \tag{23}$$

In particular, when $m_{N_R^1} = m_{N_R^2}$ ($= m_{N_R}$), the expression in Eq. (23) is reduced to

$$\begin{aligned} B(\mu \to eee) = {} & \frac{1}{64G_F^2}\left(\frac{1}{16\pi^2}\right)^2 \left(\frac{1}{m_N^2 - m_S^2}\right)^4 \left| \sum_{\alpha,\beta=1}^{2} h_\mu^{\alpha *} h_e^\alpha h_e^{\beta *} h_e^\beta \left(m_N^2 + m_S^2 - \frac{2m_N^2 m_S^2}{m_N^2 - m_S^2} \log\frac{m_N^2}{m_S^2} \right) \right. \\ & \left. + 2m_N^2 \sum_{\alpha,\beta=1}^{2} h_\mu^{\alpha *} h_e^{\alpha *} h_e^\beta h_e^\beta \left(\frac{m_N^2 + m_S^2}{m_N^2 - m_S^2} \log\frac{m_N^2}{m_S^2} - 2 \right) \right|^2. \end{aligned} \tag{24}$$

Notice that the contributions of the two diagrams to $\mu \leftrightarrow eee$ are constructive for all the parameter sets in Table II. We also note that there are additional contributions to $\mu \leftrightarrow eee$ from penguin diagrams, which are neglected because their contributions are much smaller.

[1]The formula of Eq. (22) is different from Eq. (A3) in Ref. [18] which includes errors. We have recalculated the values of $B(\mu \to e\gamma)$ by using the corrected formula and checked that the values of $B(\mu \to e\gamma)$ in the parameter sets in Table II in Ref. [18] are still below the experimental bound.

TABLE II. Values of h_i^α as well as those of branching ratios of $\mu \to e\gamma$ and $\mu \to 3e$ for $m_\eta = 50$ GeV and $m_{H^\pm} = 100$ GeV for various scenarios which satisfy neutrino data: set A and set B are scenarios of the normal hierarchy while set C and set D are those of the inverted hierarchy. For all sets, $m_S = 400$ GeV and $m_{N_R} = 5$ TeV are taken.

	Inputs		Yukawa couplings						LFV	
Set	$\sin^2\theta_{13}$	$\kappa \tan\beta$	h_e^1	h_e^2	h_μ^1	h_μ^2	h_τ^1	h_τ^2	$B(\mu \to e\gamma)$	$B(\mu \to 3e)$
A	0	54	1.2	1.3	0.024	−0.011	0.000 71	−0.0014	2.8×10^{-14}	7.8×10^{-13}
B	0.03	76	1.1	1.1	0.0028	0.018	−0.000 55	0.000 97	6.1×10^{-14}	9.8×10^{-13}
C	0	80	3.500	3.474	0.012 00	−0.011 92	−0.000 713 6	0.000 708 6	4.4×10^{-17}	8.2×10^{-14}
D	0.03	128	2.1	2.2	0.0064	−0.0086	−0.000 53	0.000 35	3.5×10^{-15}	9.3×10^{-13}

Assuming that $h_e^\alpha \sim \mathcal{O}(1)$, the masses of N_R^α and $S^\pm$ are strongly constrained from below. In particular, if we assume that $m_S \gtrsim 400$ GeV, $m_{N_R} \gtrsim \mathcal{O}(1)$ TeV is required to satisfy the current experimental bounds, $B(\mu \to e\gamma) < 1.2 \times 10^{-11}$ [28] and $B(\mu \to eee) < 1.0 \times 10^{-12}$ [27]. Such a relatively heavier $S^\pm$ is favored from the discussion on the dark matter relic abundance and electroweak baryogenesis [7,18].

D. Typical scenarios

In Table II, we show four choices for the parameter sets, and resulting values for the neutrino Yukawa coupling constants h_i^α which satisfy the neutrino data and the LFV data. For all parameter sets, $m_S = 400$ GeV and $m_{N_R} = 5$ TeV are assumed. Set A and set B are taken as the normal hierarchy in the neutrino masses with $\sin^2\theta_{13} = 0$ and 0.03, respectively, while set C and set D are for the inverted hierarchy. The predictions on $B(\mu \to e\gamma)$ and $B(\mu \to eee)$ are also shown in the table.[2] The scenario with the inverted hierarchy requires the larger values for $\kappa \tan\beta$, so that the normal hierarchy scenarios are more natural in our model.

In Fig. 3, the contour plots of the branching ratio $B(\mu \to e\gamma)$ are shown in the m_S-m_{N_R} plane for the neutrino Yukawa coupling constants in set A to set D, while those of the branching ratio $B(\mu \to eee)$ are shown for these scenarios in Fig. 4. The scale of the branching ratio of $\mu \to e\gamma$ is determined by m_{N_R} and is insensitive to m_S, while that of $\mu \to eee$ largely depend on both m_{N_R} and m_S especially for set A, set B, and set D. It can easily be seen that a much stronger constraint comes from $\mu \to eee$ for all scenarios.

E. Dark matter and electroweak phase transition

From now on, we employ set A in Table II for further phenomenological analyses. In this scenario, masses of N_R^α are at the multi-TeV scale, so that it may be natural that the rest Z_2-odd neutral field η is the candidate of dark matter. Since η is a singlet under the SM gauge group, the interactions with Z_2-even particles are only through the Higgs coupling. When $m_\eta < m_W$, the η field predominantly annihilates into $b\bar{b}$ and $\tau^+\tau^-$ through s-channel Higgs boson (h and H) mediations. Strong annihilation occurs at $m_\eta \simeq m_H/2$ (and $m_\eta \simeq m_h/2$) due to the resonance of H (h) mediation in the s-channel diagrams. The pair annihilation into two photons through one-loop diagrams by $H^\pm$ and $S^\pm$ can also be important if κ is of the order one. The relic abundance becomes consistent with the data ($\Omega_{\rm DM}h^2 \sim 0.11$ [36]) for $m_\eta \sim 50$–60 GeV, when we take $m_H = m_{H^\pm} \simeq 100$ GeV, $m_h \simeq 120$ GeV, $m_S \gtrsim 400$ GeV with $\kappa = 1.5$, $\sigma_1 = 0.05$, $\sigma_2 = 0.03$, and $\tan\beta = 36$. In such a scenario, the typical spin-independent cross section for the scattering of dark matter with a proton is of the order of 10^{-8} pb which is within the reach of the direct search experiments such as superCDMS and XMASS.

When $m_\eta < m_h/2$, the (SM-like) Higgs boson h can decay into a dark matter pair $\eta\eta$. The branching ratio of $h \to \eta\eta$ is evaluated as 34% (22%) for $m_h = 120$ GeV and $m_\eta = 48$ (55) GeV when $\sigma_1 = 0.05$, $\sigma_2 = 0.03$, and $\tan\beta > 10$. The invisible decay of h can be tested at the LHC when $B(h \to \eta\eta) > 25\%$ [37]. At the ILC, it is expected that the branching ratio for the invisible decay of a few % can be detected [38]. Therefore, the invisible decay in this model can be tested at the collider experiments.

Our model [7] satisfies the conditions for baryogenesis [8]. The B number violating interaction is the sphaleron interaction. The additional CP violating phases are in the Higgs sector and in the Yukawa interaction. The condition of departure from thermal equilibrium can be realized by the strong first order electroweak phase transition, which requires a large trilinear coupling of the order parameter in the expression of the high temperature expansion [39] where only the bosonic loop can contribute.[3] In our model, there are many additional scalars running in the loop so that the large coupling can be easily realized [17]. The strong first order phase transition is possible for large

[2] In Table II, we show the numbers of the h_i^α coupling constants with four digits for set C, because the branching ratios of $\mu \to e\gamma$ and $\mu \to eee$ are sensitive to these numbers due to large cancellations.

[3] We note that such a nondecoupling effect due to the bosonic loop can also affect the quantum correction to the triple Higgs boson coupling [17,40]. Such a large correction to the Higgs self-coupling can be an important signature for successful electroweak baryogenesis at collider experiments.

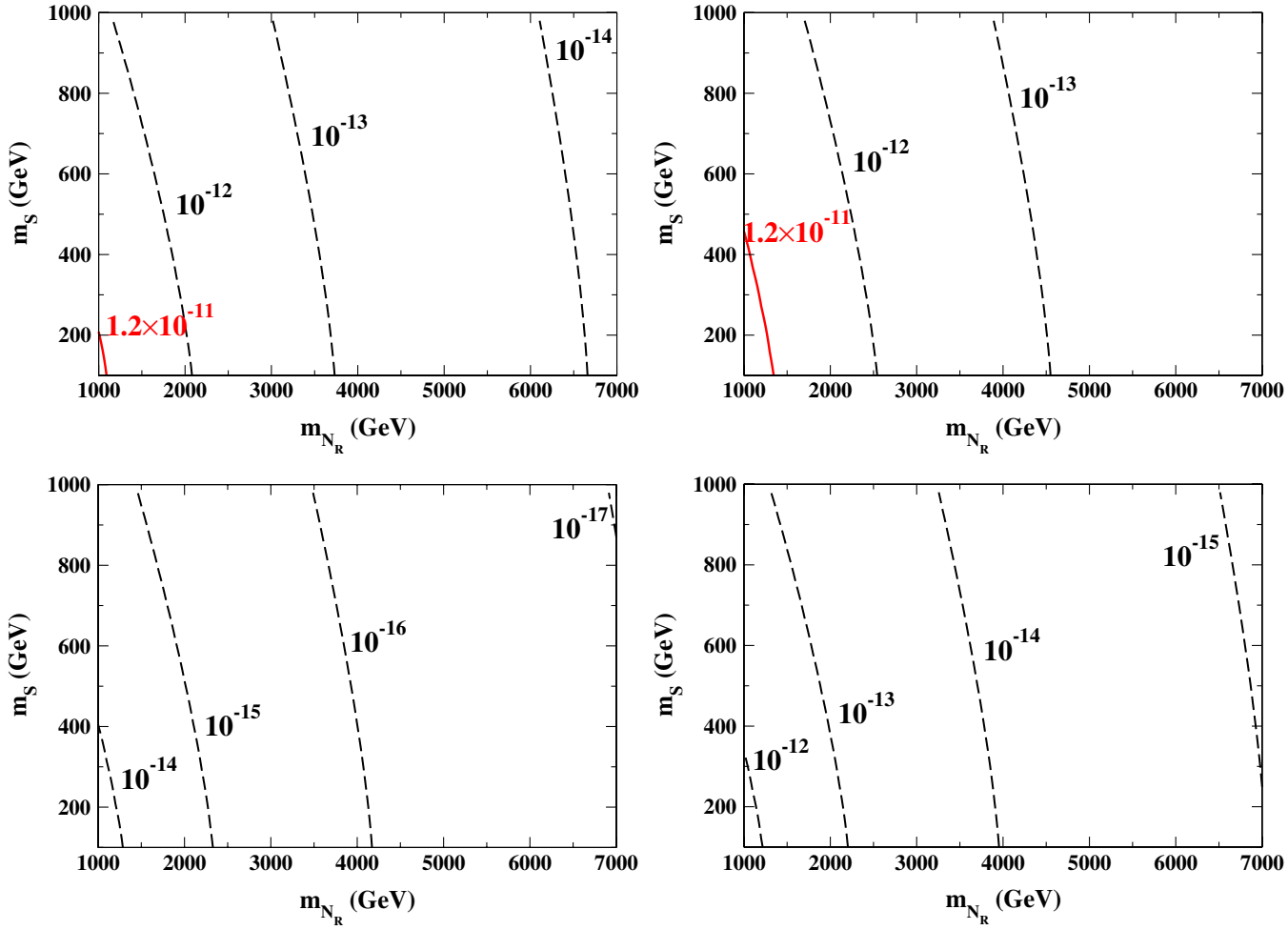

FIG. 3 (color online). Contour plots for the branching ratio of $\mu \to e\gamma$ for the neutrino Yukawa coupling constants in set A (top left), set B (top right), set C (bottom left), and set D (bottom right). The contour for the upper limit from the data is given as the (red) solid curve.

m_S and/or m_A with the large nondecoupling effect: e.g. $m_S \sim 400$ GeV, $m_A \sim 100$ GeV, $M = 100$ GeV, and $\mu_S = 200$ GeV, where M and μ_S are the invariant masses in Eqs. (7) and (11), respectively. The result is not sensitive to $\tan\beta$.

III. BOUNDS FROM TRIVIALITY AND VACUUM STABILITY

There are scalar bosons in this model, so that quadratic divergences appear in the one-loop calculation for their masses. Because there is no mechanism by which such quadratic divergences are eliminated, enormous fine-tuning is required to realize the renormalized Higgs boson mass being at the weak scale with a very high cutoff scale. Allowing the 1% fine-tuning, the cutoff scale is at most $\Lambda \sim O(10)$ TeV, above which the theory would be replaced by a more fundamental one [24]. Unless a mechanism of cancellation of the quadratic divergences such as supersymmetry is implemented, to avoid excessive fine-tuning the model should be regarded as an effective theory, whose cutoff scale Λ is between $m_{N_R^\alpha}$ and $O(10)$ TeV. We then need to confirm the theoretical consistency of the model up to Λ [23]. We here evaluate bounds on the parameter space from vacuum stability and perturbativity, and examine whether the theoretically allowed parameter region is consistent with that by the experimental data discussed in the previous sections.

We have to consider these two bounds seriously because of the following reasons. First, this model includes many scalar fields, e.g., h, H, A, $H^\pm$, $S^\pm$, and η, so that the scale dependent dimensionless coupling constants would be drastically changed by the loop corrections due to the scalar bosons. Second, some of the Yukawa coupling constants for right-handed neutrinos are necessarily of order one for a radiative generation of the tiny mass scale of the neutrinos at the three-loop level. Finally, to realize the first order electroweak phase transition, some of the scalar self-coupling constants have to be as large as of order one.

In order to evaluate the vacuum stability bound and the triviality bound, we estimate the scale dependences of the dimensionless coupling constants by using the RGEs at the one-loop level. We have calculated the one-loop beta

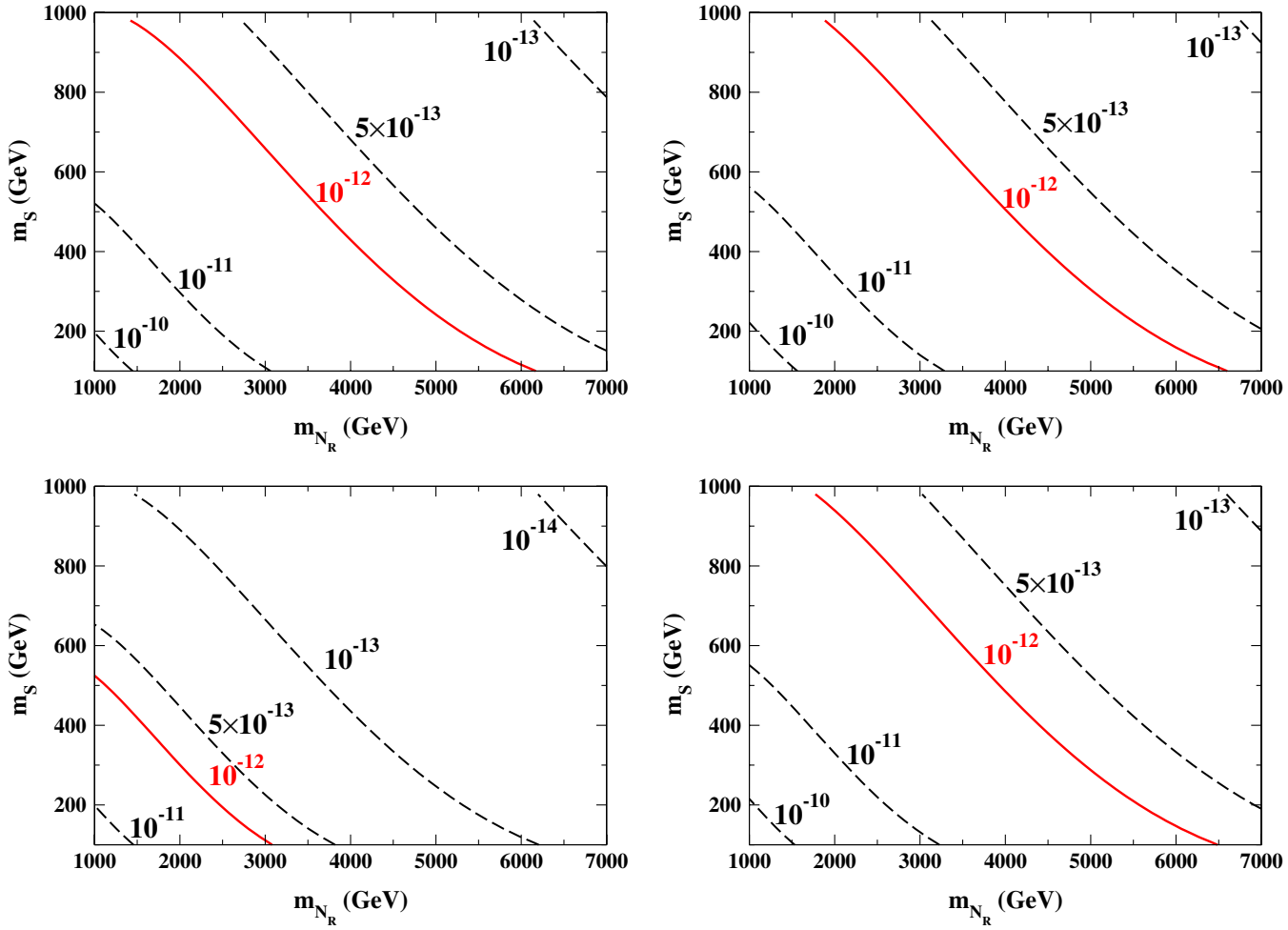

FIG. 4 (color online). Contour plots for the branching ratio of $\mu \to eee$ for the neutrino Yukawa coupling constants in set A (top left), set B (top right), set C (bottom left), and set D (bottom right). The contour for the upper limit from the data is given as the (red) solid curve.

functions for all the coupling constants in this model. The full set of the beta functions is listed in the Appendix. We take into account the threshold effects in the calculation of the scale dependent coupling constants. In the scale below the mass of $S^{\pm}$, we treat the theory without N_R and $S^{\pm}$. In the scale between the masses of the $S^{\pm}$ and N_R, we treat the theory without N_R. In the scale higher than the mass of the N_R, we treat the theory with full particle contents.

A. The conditions

In this model, there are scalar fields Φ_i $(i = 1, 2)$, $S^{\pm}$ and η, which contain 11 degrees of freedom which would share the order parameter. The four of them are eliminated because of the $SU(2)_L \times U(1)_Y$ gauge symmetry. In the remaining seven-dimensional parameter space, we require that for any direction the potential is bounded from below with keeping positiveness [41]. In the SM, this requirement is satisfied when the Higgs self-coupling constant is positive. In this model, we put the following conditions on the dimensionless coupling constants:

$$\lambda_1(\mu) > 0, \qquad \lambda_2(\mu) > 0, \qquad \lambda_S(\mu) > 0, \qquad \lambda_\eta(\mu) > 0, \tag{25}$$

$$\begin{aligned}
&\sqrt{\lambda_1(\mu)\lambda_2(\mu)} + \lambda_3(\mu) + \min[0,\ (\lambda_4(\mu) \\
&\quad + \lambda_5(\mu)),\ (\lambda_4(\mu) - \lambda_5(\mu))] > 0, \\
&\sqrt{\lambda_1(\mu)\lambda_S(\mu)/2} + \rho_1(\mu) > 0, \\
&\sqrt{\lambda_1(\mu)\lambda_\eta(\mu)/3} + \sigma_1(\mu) > 0, \\
&\sqrt{\lambda_2(\mu)\lambda_S(\mu)/2} + \rho_2(\mu) > 0, \\
&\sqrt{\lambda_2(\mu)\lambda_\eta(\mu)/3} + \sigma_2(\mu) > 0, \\
&\sqrt{\lambda_S(\mu)\lambda_\eta(\mu)/6} + \xi(\mu) > 0,
\end{aligned} \tag{26}$$

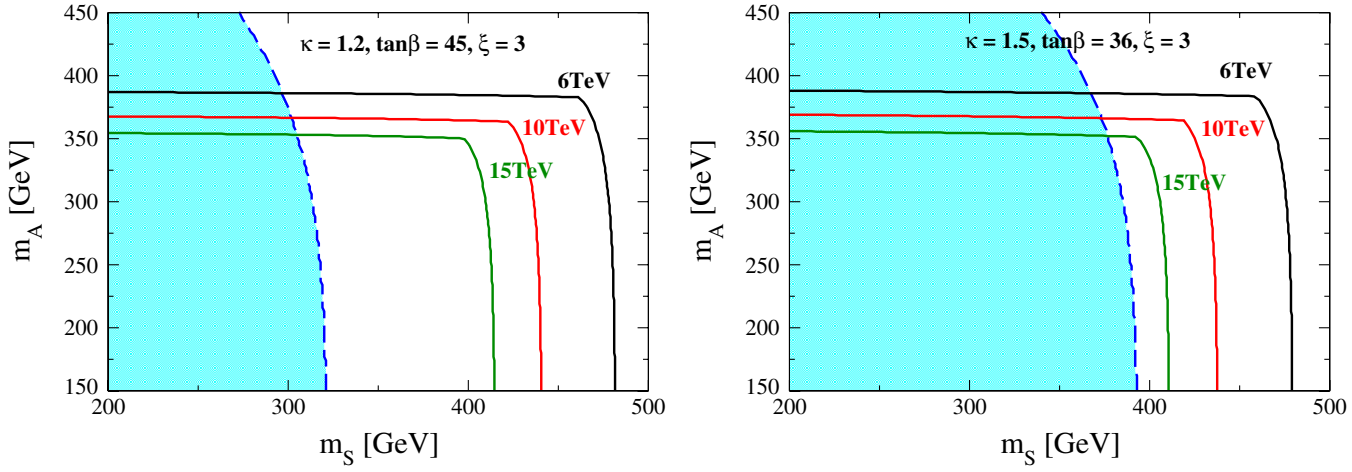

FIG. 5 (color online). Contour plots for the scale where condition of perturbativity is broken are shown in the m_S-m_A plane in the case of $(\kappa, \tan\beta) = (1.2, 45)$ (left figure), and $(\kappa, \tan\beta) = (1.5, 36)$ (right figure). The region excluded by the vacuum stability condition is also shown as the shaded area. The constant ξ is taken to be 3 at the scale of m_S.

$$2\lambda_1(\mu) + 2\lambda_2(\mu) + 4\lambda_3(\mu) + 4\rho_1(\mu) + 4\rho_2(\mu) + \lambda_S(\mu) + 4\sigma_1(\mu) + 4\sigma_2(\mu) + \tfrac{2}{3}\lambda_\eta(\mu) + 4\xi(\mu) - 16\sqrt{2}|\kappa(\mu)| > 0. \quad (27)$$

The conditions in Eqs. (25) and (26) are obtained by the similar way as in Ref. [11], while the last condition in Eq. (27) is derived such that the term with the coupling constant κ in the potential satisfies the positivity condition for the direction where the VEVs of the fields Φ_1, Φ_2, $S^\pm$, and η are a common value.

We require that all the dimensionless running coupling constants do not blow up below Λ. Since we discuss the model within the scale where the perturbation calculation remains reliable, we here require that the running coupling constants do not exceed some critical value. In this paper, we impose the following criterion in the coupling constants in the Higgs potential Eq. (7) and the Yukawa interaction in Eqs. (1) and (2):

$$|\lambda_i(\mu)|,\ |\sigma_i(\mu)|,\ |\rho_i(\mu)|,\ |\kappa(\mu)|,\ |\xi(\mu)| < 8\pi,$$
$$y_t^2(\mu),\ y_b^2(\mu),\ y_\tau^2(\mu),\ (h_i^\alpha)^2(\mu) < 4\pi. \quad (28)$$

The similar critical value has been adopted in the analyses in the two Higgs doublet model [26] and in the Zee model [11].

TABLE III. Values for the scalar boson masses and the invariant mass parameters.

Masses (GeV)				Invariant masses (GeV)		
$m_H^\pm$	m_H	m_h	m_η	M	μ_S	μ_η
100	100	120	50	100	200	30

B. Allowed regions in the parameter space

In this section, we evaluate allowed regions in parameter space, which satisfy the conditions of triviality and vacuum stability for each fixed cutoff scale Λ. For the scenarios of the neutrino Yukawa coupling constants as well as the masses of right-handed neutrinos, we choose set A in Table II. We investigate the allowed regions in the m_S-m_A plane, and the rest of the mass parameters in the scalar sector are fixed as shown in Table III.

The initial values for the scalar coupling constants in the Higgs sector are shown in Table. IV. We note that the initial values of λ_4, λ_5, and ρ_2 are determined by given values for the masses of A and $S^\pm$ using Eqs. (7), (8), and (11). The rest parameter ξ (the coupling constant for $|S^-|^2\eta^2$) is taken as $\xi = 3$ and 5. The results in the case with $\xi = 3$ are shown in Fig. 5 for $\kappa = 1.2$ (left figure) and $\kappa = 1.5$ (right figure), while those with $\xi = 5$ is in Fig. 6 for the same values of κ.

In Fig. 5, the shaded area in the figure is excluded due to the vacuum stability condition in Eq. (27). In this area, the

TABLE IV. Values for the scalar coupling constants and the mixing angles.

Scalar couplings									
$\lambda_1(m_Z)$	$\lambda_2(m_Z)$	$\lambda_3(m_Z)$	$\kappa(m_S)\tan\beta$	$\rho_1(m_S)$	$\lambda_S(m_S)$	$\sigma_1(m_Z)$	$\sigma_2(m_Z)$	$\lambda_\eta(m_Z)$	$\sin(\beta-\alpha)$
0.24	0.24	0.24	54	0.1	2	0.05	0.05	3	1

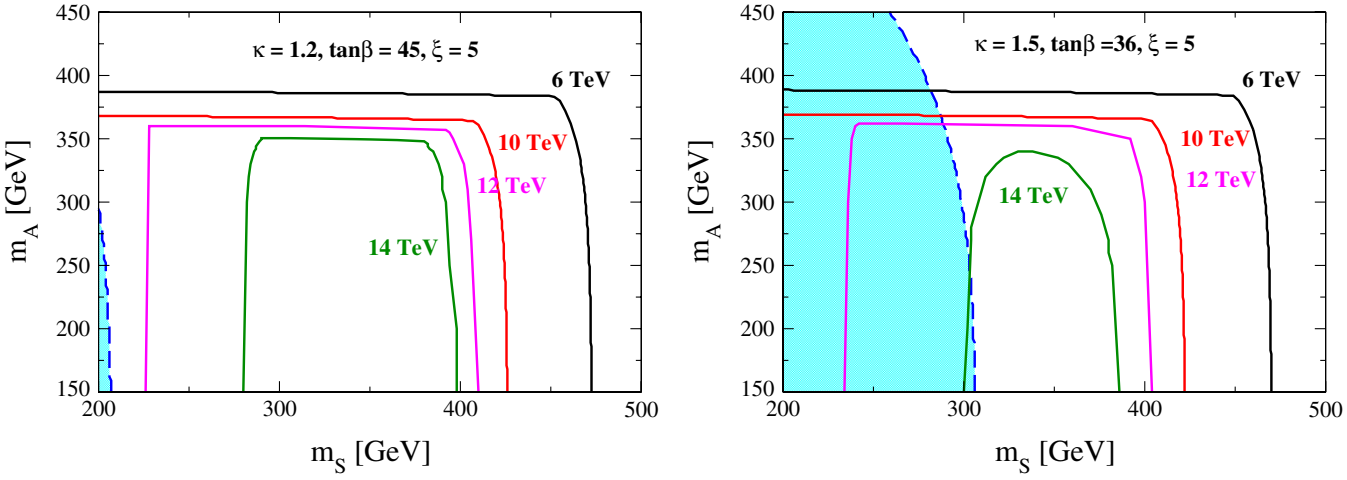

FIG. 6 (color online). Contour plots for the scale where condition of perturbativity is broken are shown in the m_S-m_A plane in the case of $(\kappa, \tan\beta) = (1.2, 45)$ (left figure), and $(\kappa, \tan\beta) = (1.5, 36)$ (right figure). The region excluded by the vacuum stability condition is also shown as the shaded area. The constant ξ is taken to be 5 at the scale of m_S.

condition is not satisfied already at the electroweak scale, so that the excluded region is independent of Λ. The vacuum stability bound becomes stronger for a larger value of κ, although the area compatible with both theoretical conditions with $\Lambda = 10$ TeV still exists for $\kappa = 1.5$. On the other hand, the bound from perturbativity depends on Λ. In Fig. 5, the contour plots for $\Lambda = 6$, 10, and 15 TeV, the scales where one of the coupling constants blows up and breaks the condition of perturbativity are shown for the case of $\xi = 3$ in the m_S-m_A plane. We find that there is the parameter region which satisfies both the conditions of vacuum stability and perturbativity with the blow-up scale to be above $\Lambda = 10$ TeV. The area of the vicinity of $m_S \sim 400$ GeV and $m_A < 350$ GeV can also be consistent from the theoretical bounds. We stress that this parameter region is favored for phenomenologically successful scenarios for neutrino masses, relic abundance for the dark matter, and the strongly first order phase transition.

The similar figures but with $\xi = 5$ are shown in Fig. 6. The contour plots are for $\Lambda = 6$, 10, 12, and 14 TeV in the m_S-m_A plane. We find that there is the parameter region which satisfies both the conditions of vacuum stability and perturbativity with the blow-up scale to be above $\Lambda = 10$ TeV. The vacuum stability bound is more relaxed as compared to that for $\xi = 3$, while the bound from perturbativity becomes rather strict. In the regions with $m_S < 400$ GeV, the running coupling constants blow up earlier than the case with $\xi = 3$, because of the threshold effect at the scale $\mu = m_S$, above which the running of λ_η becomes enhanced by the loop contribution of $S^\pm$. In the area of 300 GeV $< m_S <$ 400 GeV and $m_A < 350$ GeV, Λ can be above 10 TeV.

IV. CONCLUSION

We have discussed theoretical constraints on the parameter space under the conditions from vacuum stability and triviality in the three-loop radiative seesaw model with TeV-scale right-handed neutrinos which are odd under the Z_2 parity. It has been found that the model can be consistent up to the scale above 10 TeV in the parameter region which satisfies the neutrino data, the LFV data, the thermal relic abundance of dark matter as well as the requirement from the strongly first order phase transition. We also reanalyzed the constraint from the LFV data. The data from $\mu \to eee$ is found to be more severe than that from $\mu \to e\gamma$. Our analysis here has been restricted in the case where the CP violation is neglected just for simplicity. The analysis for consistency with including the CP violating phase, which is necessary for finally producing the observed asymmetry of baryon number at the electroweak phase transition, will be done in the near future.

ACKNOWLEDGMENTS

We would like to thank Toru Goto for indicating the importance of the $\mu \to eee$ process in our model. The work of M. A. was supported in part by Grant-in-Aid for Young Scientists (B) No. 22740137, that of S. K. was supported in part by Grant-in-Aid for Scientific Research (A) No. 22244031 and (C) No. 19540277, and that of K. Y. was supported by Japan Society for the Promotion of Science (JSPS Fellow (DC2)).

APPENDIX

The full set of the beta functions for RGEs in the model in Ref. [7] is given at the one-loop level by

$$\beta(g_s) = \frac{1}{16\pi^2}[-7g_s^3], \tag{A1}$$

$$\beta(g) = \frac{1}{16\pi^2}[-3g^3], \tag{A2}$$

$$\beta(g') = \frac{1}{16\pi^2}\left[-\frac{22}{3}g'^3\right], \tag{A3}$$

$$\beta(y_t) = \frac{1}{16\pi^2}\left[-8y_t g_s^2 - \frac{9}{4}g^2 y_t - \frac{17}{12}g'^2 y_t + \frac{9}{2}y_t^3 + \frac{3}{2}y_t y_b^2\right], \tag{A4}$$

$$\beta(y_b) = \frac{1}{16\pi^2}\left[-8y_t g_s^2 - \frac{9}{4}g^2 y_t - \frac{5}{12}g'^2 y_t + \frac{9}{2}y_b^3 + \frac{3}{2}y_t^2 y_b\right], \tag{A5}$$

$$\beta(y_\tau) = \frac{1}{16\pi^2}\left[-\frac{9}{4}g^2 y_\tau - \frac{15}{4}g'^2 y_\tau + \frac{5}{2}y_\tau^3\right], \tag{A6}$$

$$\beta(h_i^\alpha) = \frac{1}{16\pi^2}\left[-5g'^2 h_i^\alpha + \frac{1}{2}h_i^\alpha \sum_j (h_j^\alpha)^2 + \frac{1}{2}h_i^\alpha \sum_\beta (h_i^\beta)^2 + h_i^\alpha \sum_{j,\beta} (h_j^\beta)^2\right], \tag{A7}$$

$$\beta(\lambda_1) = \frac{1}{16\pi^2}\left[12\lambda_1^2 + 4\lambda_3^2 + 2\lambda_4^2 + 2\lambda_5^2 + 4\lambda_3\lambda_4 + 2\rho_1^2 + \sigma_1^2 + \frac{9}{4}g^4 + \frac{6}{4}g^2 g'^2 + \frac{3}{4}g'^4 - 4y_\tau^4 + (4y_\tau^2 - 9g^2 - 3g'^2)\lambda_1\right], \tag{A8}$$

$$\beta(\lambda_2) = \frac{1}{16\pi^2}\left[12\lambda_2^2 + 4\lambda_3^2 + 2\lambda_4^2 + 2\lambda_5^2 + 4\lambda_3\lambda_4 + 2\rho_2^2 + \sigma_2^2 + \frac{9}{4}g^4 + \frac{6}{4}g^2 g'^2 + \frac{3}{4}g'^4 - 12y_t^4 - 12y_b^4 + (12y_t^2 + 12y_b^2 - 9g^2 - 3g'^2)\lambda_2\right], \tag{A9}$$

$$\beta(\lambda_3) = \frac{1}{16\pi^2}\left[6\lambda_1\lambda_3 + 2\lambda_1\lambda_4 + 6\lambda_2\lambda_3 + 2\lambda_2\lambda_4 + 4\lambda_3^2 + 2\lambda_4^2 + 2\lambda_5^2 + 2\rho_1\rho_2 + \sigma_1\sigma_2 + 4\kappa^2 + \frac{9}{4}g^4 + \frac{3}{4}g'^4 - \frac{6}{4}g^2 g'^2 + (6y_t^2 + 6y_b^2 + 2y_\tau^2 - 9g^2 - 3g'^2)\lambda_3\right], \tag{A10}$$

$$\beta(\lambda_4) = \frac{1}{16\pi^2}[2(\lambda_1 + \lambda_2 + 4\lambda_3 + 2\lambda_4)\lambda_4 + 8\lambda_5^2 - 8\kappa^2 + 3g^2 g'^2 + (6y_t^2 + 6y_b^2 + 2y_\tau^2 - 9g^2 - 3g'^2)\lambda_4], \tag{A11}$$

$$\beta(\lambda_5) = \frac{1}{16\pi^2}[2(\lambda_1 + \lambda_2 + 4\lambda_3 + 6\lambda_4)\lambda_5 + (6y_t^2 + 6y_b^2 + 2y_\tau^2 - 9g^2 - 3g'^2)\lambda_5] \tag{A12}$$

$$\beta(\rho_1) = \frac{1}{16\pi^2}\left[6\lambda_1\rho_1 + 4\lambda_3\rho_2 + 2\lambda_4\rho_2 + 2\rho_1\lambda_S + 4\rho_1^2 + \sigma_1\xi + 8\kappa^2 + 3g'^4 + \left(-\frac{15}{2}g'^2 - \frac{9}{2}g^2 + 2\sum_{i,\alpha}(h_i^\alpha)^2 + 2y_\tau^2\right)\rho_1\right], \tag{A13}$$

$$\beta(\rho_2) = \frac{1}{16\pi^2}\left[6\lambda_2\rho_2 + 4\lambda_3\rho_1 + 2\lambda_4\rho_1 + 2\rho_2\lambda_S + 4\rho_2^2 + \sigma_2\xi + 8\kappa^2 + 3g'^4 + \left(-\frac{15}{2}g'^2 - \frac{9}{2}g^2 + 2\sum_{i,\alpha}(h_i^\alpha)^2 + 6y_t^2 + 6y_b^2\right)\rho_2\right], \tag{A14}$$

$$\beta(\lambda_S) = \frac{1}{16\pi^2}\left[8\rho_1^2 + 8\rho_2^2 + 5\lambda_S^2 + 2\xi^2 + 24g'^4 - 12g'^2\lambda_S + 4\sum_{i,\alpha}(h_i^\alpha)^2\lambda_S - 8\sum_{i,j}\sum_{\alpha,\beta} h_i^\alpha h_i^\beta h_j^\beta h_j^\alpha\right], \tag{A15}$$

$$\beta(\sigma_1) = \frac{1}{16\pi^2}\left[6\lambda_1\sigma_1 + (4\lambda_3 + 2\lambda_4)\sigma_2 + \sigma_1\lambda_\eta + 2\rho_1\xi + 16\kappa^2 + \left(-\frac{9}{2}g^2 - \frac{3}{2}g'^2 + 2y_\tau^2\right)\sigma_1\right], \tag{A16}$$

$$\beta(\sigma_2) = \frac{1}{16\pi^2}\left[6\lambda_2\sigma_2 + (4\lambda_3 + 2\lambda_4)\sigma_1 + \sigma_2\lambda_\eta + 2\rho_2\xi + 16\kappa^2 + \left(-\frac{9}{2}g^2 - \frac{3}{2}g'^2 + 6y_t^2 + 6y_b^2\right)\sigma_2\right], \tag{A17}$$

$$\beta(\lambda_\eta) = \frac{1}{16\pi^2}[12(\sigma_1^2 + \sigma_2^2) + 3\lambda_\eta^2 + 6\xi^2], \tag{A18}$$

$$\beta(\kappa) = \frac{1}{16\pi^2}\kappa\left[2\lambda_3 - 2\lambda_4 + 2\xi + 2\sigma_1 + 2\sigma_2 + 2\rho_1 + 2\rho_2 + \sum_{\alpha,i}(h_i^\alpha)^2 - \frac{9}{2}g^2 - \frac{9}{2}g'^2 + 3y_t^2 + 3y_b^2 + y_\tau^2\right], \tag{A19}$$

$$\beta(\xi) = \frac{1}{16\pi^2}\left[4\rho_1\sigma_1 + 4\rho_2\sigma_2 + 2\lambda_S\xi + \lambda_\eta\xi + 4\xi^2 - 6g'^2\xi + 2\sum_{\alpha,i}(h_i^\alpha)^2\xi\right]. \tag{A20}$$

[1] M. C. Bento, O. Bertolami, R. Rosenfeld, and L. Teodoro, Phys. Rev. D **62**, 041302 (2000).

[2] X. G. He, T. Li, X. Q. Li, J. Tandean, and H. C. Tsai, Phys. Lett. B **688**, 332 (2010); M. Farina, D. Pappadopulo, and A. Strumia, Phys. Lett. B **688**, 329 (2010); K. Cheung and T. C. Yuan, Phys. Lett. B **685**, 182 (2010); S. Kanemura, S. Matsumoto, T. Nabeshima, and N. Okada, Phys. Rev. D **82**, 055026 (2010).

[3] A. Zee, Phys. Lett. **93B**, 389 (1980); **95B**, 461(E) (1980); **161B**, 141 (1985).

[4] A. Zee, Nucl. Phys. **B264**, 99 (1986); K. S. Babu, Phys. Lett. B **203**, 132 (1988).

[5] L. M. Krauss, S. Nasri, and M. Trodden, Phys. Rev. D **67**, 085002 (2003).

[6] E. Ma, Phys. Rev. D **73**, 077301 (2006).

[7] M. Aoki, S. Kanemura, and O. Seto, Phys. Rev. Lett. **102**, 051805 (2009).

[8] A. D. Sakharov, Pis'ma Zh. Eksp. Teor. Fiz. **5**, 32 (1967).

[9] For example, A. G. Cohen, D. B. Kaplan, and A. E. Nelson, Annu. Rev. Nucl. Part. Sci. **43**, 27 (1993); M. Quiros, Helv. Phys. Acta **67**, 451 (1994); V. A. Rubakov and M. E. Shaposhnikov, Phys. Usp. **39**, 461 (1996) [Usp. Fiz. Nauk **166**, 493 (1996)].

[10] J. Kubo, E. Ma, and D. Suematsu, Phys. Lett. B **642**, 18 (2006); T. Hambye, K. Kannike, E. Ma, and M. Raidal, Phys. Rev. D **75**, 095003 (2007); D. Aristizabal Sierra, J. Kubo, D. Restrepo, D. Suematsu, and O. Zapata, Phys. Rev. D **79**, 013011 (2009).

[11] S. Kanemura, T. Kasai, G. L. Lin, Y. Okada, J. J. Tseng, and C. P. Yuan, Phys. Rev. D **64**, 053007 (2001).

[12] K. S. Babu and C. Macesanu, Phys. Rev. D **67**, 073010 (2003); D. Aristizabal Sierra and M. Hirsch, J. High Energy Phys. 12 (2006) 052; M. Nebot, J. F. Oliver, D. Palao, and A. Santamaria, Phys. Rev. D **77**, 093013 (2008).

[13] M. Aoki, S. Kanemura, T. Shindou, and K. Yagyu, J. High Energy Phys. 07 (2010) 084.

[14] K. Cheung and O. Seto, Phys. Rev. D **69**, 113009 (2004).

[15] E. Ma, Phys. Lett. B **662**, 49 (2008); E. Ma, Mod. Phys. Lett. A **23**, 721 (2008); R. A. Porto and A. Zee, Phys. Rev. D **79**, 013003 (2009); E. Ma and D. Suematsu, Mod. Phys. Lett. A **24**, 583 (2009).

[16] Q. H. Cao, E. Ma, and G. Rajasekaran, Phys. Rev. D **76**, 095011 (2007).

[17] S. Kanemura, Y. Okada, and E. Senaha, Phys. Lett. B **606**, 361 (2005).

[18] M. Aoki, S. Kanemura, and O. Seto, Phys. Rev. D **80**, 033007 (2009).

[19] M. Aoki, S. Kanemura, K. Tsumura, and K. Yagyu, Phys. Rev. D **80**, 015017 (2009).

[20] A. Belyaev, R. Guedes, S. Moretti, and R. Santos, J. High Energy Phys. 07 (2010) 051.

[21] M. Aoki and S. Kanemura, Phys. Lett. B **689**, 28 (2010).

[22] M. Aoki, S. Kanemura, and O. Seto, Phys. Lett. B **685**, 313 (2010).

[23] N. Cabibbo, L. Maiani, G. Parisi, and R. Petronzio, Nucl. Phys. **B158**, 295 (1979); K. Inoue, A. Kakuto, H. Komatsu, and S. Takeshita, Prog. Theor. Phys. **67**, 1889 (1982); H. Komatsu, Prog. Theor. Phys. **67**, 1177 (1982).

[24] C. F. Kolda, and H. Murayama, J. High Energy Phys. 07 (2000) 035.

[25] S. Kanemura, T. Kubota, and E. Takasugi, Phys. Lett. B **313**, 155 (1993); A. G. Akeroyd, A. Arhrib, and E. M. Naimi, Phys. Lett. B **490**, 119 (2000); I. F. Ginzburg and I. P. Ivanov, Phys. Rev. D **72**, 115010 (2005).

[26] S. Nie and M. Sher, Phys. Lett. B **449**, 89 (1999); S. Kanemura, T. Kasai, and Y. Okada, Phys. Lett. B **471**, 182 (1999).

[27] U. Bellgardt *et al.* (SINDRUM Collaboration), Nucl. Phys. **B299**, 1 (1988).

[28] M. L. Brooks *et al.* (MEGA Collaboration), Phys. Rev. Lett. **83**, 1521 (1999).

[29] S. L. Glashow and S. Weinberg, Phys. Rev. D **15**, 1958 (1977).

[30] V. D. Barger, J. L. Hewett, and R. J. N. Phillips, Phys. Rev. D **41**, 3421 (1990).

[31] Y. Grossman, Nucl. Phys. **B426**, 355 (1994).

[32] H. S. Goh, L. J. Hall, and P. Kumar, J. High Energy Phys. 05 (2009) 097; S. Su and B. Thomas, Phys. Rev. D **79**, 095014 (2009); H. E. Logan and D. MacLennan, Phys. Rev. D **79**, 115022 (2009).

[33] G. Passarino and M. J. G. Veltman, Nucl. Phys. **B160**, 151 (1979).

[34] Z. Maki, M. Nakagawa, and S. Sakata, Prog. Theor. Phys. **28**, 870 (1962).

[35] K. Nakamura *et al.* (Particle Data Group), J. Phys. G **37**, 075021 (2010).

[36] E. Komatsu *et al.* (WMAP Collaboration), Astrophys. J. Suppl. Ser. **180**, 330 (2009).

[37] B. Di Girolamo and L. Neukermans, Atlas Report No. ATL-PHYS-2003-006, 2003; M. Warsinsky (ATLAS Collaboration), J. Phys. Conf. Ser. **110**, 072046 (2008).

[38] M. Schumacher, Report No. LC-PHSM-2003-096.

[39] G. W. Anderson and L. J. Hall, Phys. Rev. D **45**, 2685 (1992); M. Dine, R. G. Leigh, P. Y. Huet, A. D. Linde, and D. A. Linde, Phys. Rev. D **46**, 550 (1992).

[40] S. Kanemura, S. Kiyoura, Y. Okada, E. Senaha, and C. P. Yuan, Phys. Lett. B **558**, 157 (2003); S. Kanemura, Y. Okada, E. Senaha, and C. P. Yuan, Phys. Rev. D **70**, 115002 (2004).

[41] N. G. Deshpande and E. Ma, Phys. Rev. D **18**, 2574 (1978).